Finite Element Analysis of a NORSOK L005 Ball Valve for Oil & Gas Applications

Felipe Frizon[1], Diego Rizzotto Rossetto, Diogenes Barbosa Teles[2]

[1]*Department of Mechanical Engineering, Federal Technological University of Paraná*
Via do Conhecimento, s/n - KM 01- 85503-390 - Fraron, Pato Branco /PR Brazil
frizon@alunos.utfpr.edu.br, diegorossetto@utfpr.edu.br
[2]*Micromazza, Engenharia*
BR-470, 168, Vila Flores – RS - 95334-000 – Brazil
dbteles@ucs.br

Abstract. The oil and gas sector is one of the main consumers of industrial valves, which are essential devices for managing liquid, gas, or mixed fluids, ensuring safety and production in this industry. Designed according to international standards, valves undergo structural analyses with calculations to ensure reliability and safety, considering the pipeline's pressure class. In this study, a NPS 6 trunnion-mounted split-body ball valve was analyzed, with flanged connections between the body and the cover designed according to NORSOK L005 [5] standard. Using the finite element method and ANSYS software, three analyses were applied: linear-elastic with stress linearization, elastoplastic, and elastoplastic for localized deformations, following the guidelines of ASME VIII, Division II code [7]. The study resulted in an optimized valve geometry concerning mass concentration in the body-to-cover connection, meeting the strength criteria defined in the design by analysis methodology of ASME VIII, Division II [7].

Keywords: ball valve, NORSOK L005, oil and gas industry, finite element analysis.

1 Introduction

Among the various industrial processes, the oil sector is one of the main consumers of valves. Due to the significance of these components, valves are estimated to represent 6% to 10% of the total cost of a petrochemical plant and can account for 20% to 30% of the piping cost [1]. Consequently, this sector demands high levels of sophistication and innovation in valve design, with the development of technologies aimed at cost reduction and, most importantly, safety. This is because, given the complexity of the oil industry, failures can have catastrophic economic and socio-environmental consequences [2]

The oil and gas industry extensively utilizes ball valves due to their ability to handle powerful fluids and gases that require rapid and secure shut-off. These valves offer reliable sealing when closed, low pressure drop, as well as precise and fast opening and closing. For the sizing of these valves, internationally applicable standards such as ASME B16.34 [3] and API 6D [4] are used. Additionally, in specific regions like the North Sea region, some clients also adopt additional standards, such as NORSOK [5]. These standards constitute a set of guidelines developed by the Norwegian oil and gas industry to ensure projects applied to the oil and gas sector have appropriate safety, value addition, and an optimal cost-benefit ratio [6].

The NORSOK L005 [5] standard provides design criteria for compact flanges, enabling weight and size reduction compared to conventional flanges. Ball valves used in the oil and gas sector have flanged connections between the body and cover, and adopting the NORSOK L005 [5] standard allows for cost reduction in manufacturing, as this joint is one of the areas with the highest mass concentration in the entire component.

In addition to the valve sizing methodology based on standardized equations, the ASME VIII Division II [7] presents the design by analysis methodology, which aims to safeguard against plastic collapse using elastic stress, limit load, and elastoplastic stress methods. It also considers localized failures through the elastic stress method and the elastoplastic deformation method. Moreover, cyclic failures are examined using the fatigue analysis method.

This article focuses on sizing a NPS6, Class 600, trunnion-mounted split-body ball valve based on the criteria outlined in NORSOK L005 [5] for its body-to-cover joint. Following the design principles, a numerical model will be created using the finite element method, employing the commercial software ANSYS. This model will facilitate analyses encompassing elastic stresses using stress linearization, as well as elastoplastic stresses and localized elastoplastic deformations. The ultimate goal is to derive a ball valve geometry that meets structural collapse resistance requirements, effectively prevents local failures with an acceptable safety margin, and verifies the applicability of NORSOK L005 in the design of body and cover flanges.

2 Case study of ball valve sizing by NORSOK L005

2.1 Design by analysis – finite elements method

The ANSYS Workbench R2018 software was used as a computational tool for the methods of elastic analysis, elastoplastic analysis, and localized deformations, including pre-processing, processing, and post-processing, through the static-structural module. For defining the material curve, stress linearization, results handling, and graph plotting, the Python 3 programming language compiled in the Spyder IDE was used.

To reduce computational cost, the valve analysis was simplified by considering only half of the geometry due to its symmetry. To represent the test condition, we applied blind flanges at the ends of the valve, in the cavities of the lever and trunnion shafts, and also at the trunnion drain plug. We used linear contacts (Bonded and No Separation) for the elastic stress analysis and non-linear contacts (Bonded and Frictional) for the elastoplastic analysis.

The valve geometry and materials for each analysis were defined, followed by discretization using TET10 elements for the body, cover, and end flanges, and HEX20 elements for the nuts and bolts. For the end flanges, an automatic mesh was generated, with adjustment of element sizes, resulting in some WED15 and PYR13 elements.

The mesh was sized considering parabolic tetrahedral elements, which model variable stresses and deformations. Each element edge corresponds to ¼ of the smallest thickness of the valve, ensuring a good approximation of results with lower computational cost. The discretized model is shown in Figure 1a, the boundary conditions in Figure 1b, and Table 1 displays the mesh quality parameters.

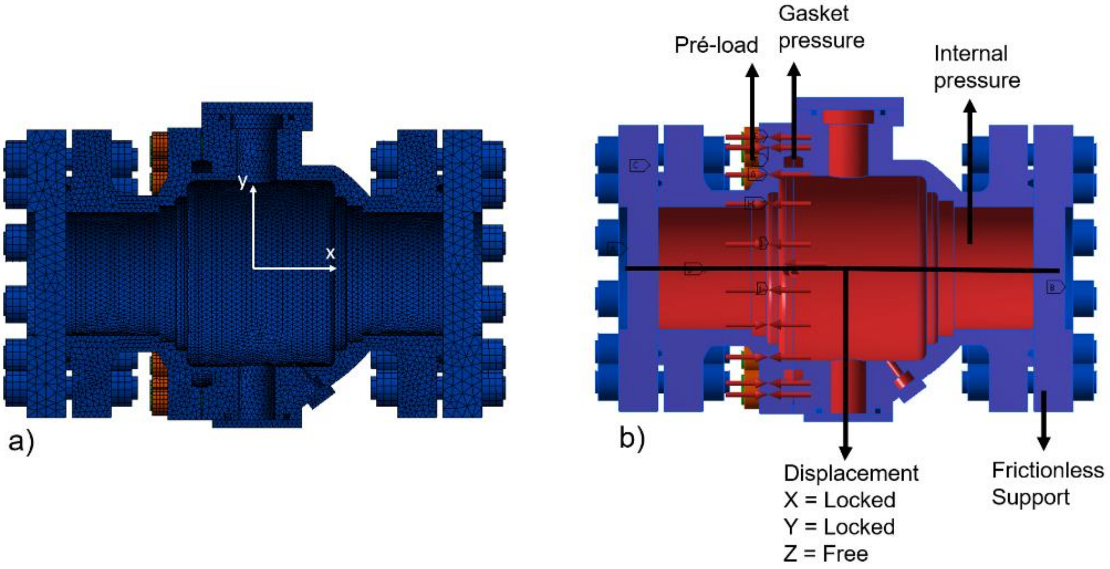

Figure 1 – a) Finite element mesh, b) Boundary conditions

Table 1- Mesh quality parameters

Parameter	Minimum	Maximum	Average	σ	Target
Element Quality	2E-2	1	0,81	0,13	1
Aspect Ratio	1	371	2,2	1,7	1
Warping	0	0,32	5E-2	5E-2	0
Orthogonal Quality	7E-6	0,99	0,75	0,15	1
Jacobian	-1	1	0,96	0,14	-1 or 1
Max. Corner Angle	64 °	176 °	98 °	14 °	90 °
Nodes			437829		
Elements			263175		

2.2 Elastic stress analysis method

For the linear elastic analysis model, constant properties of isotropic materials were used, as shown in Table 2. These properties were defined based on their respective ASTM standards and input into the software with a linear elastic behavior.

Table 2- Isotropic properties of materials used in the project.

Material	Component	Elastic modulus [GPa]	Yield stress [MPa]	Ultimate Stress [MPa]	Poisson's Ratio
ASTM A-193 GRB7	Bolts	200	720	860	0,3
ASTM A-194 GR2H	Nuts	200	720	860	0,3
ASTM A-216 GRWCB	Body and cover	200	250	570	0,3

To obtain a more accurate representation of stress variation across the thickness of the valve wall, stress linearization was employed with 16 load paths (L1 to L16) applied to regions of interest in the analysis. This allowed for a more effective identification of points with lower thickness and higher stress concentration. The boundary conditions in Figure 1 included an internal pressure of 10.34 MPa, a pre-load of 147 kN, and a joint pressure of 13.42 MPa. For the linear analyses, the values were kept constant during the analysis time.

The linear analysis was divided into two-time intervals. In the first interval, the pre-load was applied with its nominal value, while in the second interval, the pre-load was kept blocked. This condition was adopted to represent the physical behavior of this loading, which occurs only at the beginning of the analysis.

According to the guidelines of ASME VIII Division II [7], it is necessary to consider certain load combinations. In this case, the effects of pressure generated by fluid weight, wind, snow, and flow-induced moments within the pipeline were disregarded. This simplification was made because the values of these effects are two orders of magnitude smaller than the internal pressure, rendering them insignificant in terms of their impact on the results.

After processing the analysis, the values of membrane stress, bending stress, combined membrane and bending stress, peak stress, and total stress were calculated for each defined load path. Subsequently, compliance evaluations were conducted with the criteria established by ASME VIII Division II [7]. The adopted criteria can be found in Table 3, based on the material's yield strength (Sy).

Table 3 – Pass/Fail Criterion for Each Analyzed Failure Mode

Failure Mode	Pass / fail Criteria	Limit
Structural collapse	Primary Membrane Stress ≤ S	S = minimum (Sy/1.5; Sut/2.4)
	Primary Bending Stress ≤ Spl	Spl = Sy
Incremental collapse	Secondary Stress (Membrane + Bending) ≤ Sps	Sps = Sy
Fatigue	Peak ≤ Sa	Sa = Attachment 5F ASME VIII Div II
Structural collapse	Total Stress ≤ Sy	Sy

2.3 Elastic-plastic stress analysis

In a linear analysis using the finite element method, throughout the resolution of the problem, the structure's stiffness remains constant, requiring only the assembly of the initial stiffness with mesh creation. However, in various real physical problems, the stiffness varies over time, constituting nonlinearity. This variation in stiffness may occur due to geometric conditions, material properties, or specific physical behavior. To solve a nonlinear problem, it is necessary to use a stiffness corrector in the force-displacement relationship, known as the geometric stiffness matrix, which is added to the initial stiffness matrix. In this way, it is possible to observe that the method for solving a nonlinear problem is incremental, where the total applied load is divided into sequential increments applied iteratively, seeking a path of equilibrium between internal and external forces, as well as internal and external work [8].

To model the elastoplastic behavior of each material, a true stress-strain curve model was used, including temperature-dependent hardening behavior as provided in Annex 3-D of ASME VIII Division II [7] standard and data from ASME II Part D [9]. The stress and strain curves of the materials are shown in Figures 2a, 2b, and 2c.

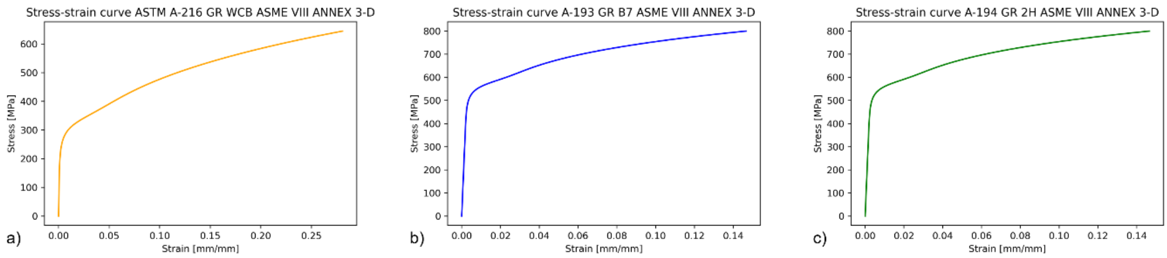

Figure 2 - Stress-strain graphs for the materials used

By using this material model, the hardening behavior was included up to the true maximum stress, and the perfect plasticity behavior (i.e., the slope of the stress-strain curves is considered zero) beyond this limit. The effects of nonlinear geometry were also considered in this analysis.

To perform the analysis with nonlinearity, a load combination was applied as shown in Equation 1. This combination was divided into 12 steps, with a minimum of 10 iterations per step and a maximum of 25 iterations. The resulting stress from gasket crushing was kept constant over time, while the pre-load, similarly to linear loads, was applied in the first-time interval and kept blocked in the subsequent intervals.

$$CMB1 = \beta(P + P_S + D), \tag{1}$$

Where β is an amplification factor adopted for this analysis as 2.4, as indicated in Table 4.1.3 of ASME VIII Division II [7], the term P represents the internal line pressure, Ps denotes the static fluid loads, and D represents the self-weight of the valve. Only this combination was considered due to the nature of the evaluated component, where wind, snow, and earthquake loads are not significant for the design.

To conduct the analysis, an iterative method with the modified Newton-Raphson solution procedure was employed. This method was chosen because it calculates only the inverse of the main diagonal of the Jacobian matrix, representing the partial derivatives of the system of equations with respect to the system variables, in each iteration. This significantly reduces the computational cost of the analysis.

For the convergence criterion, a force-based method was used, defining a tolerance of 1% for convergence, with a minimum reference value of 0.01 N. With this, the acceptance criteria of the analysis were evaluated following the item 5.2.4.3 of the standard, wherein if analysis convergence is achieved, the component is stable under the applied loads for this evaluated case. Otherwise, the component configuration (i.e., thickness) should be modified or the applied loads should be reduced, and the analysis repeated until achieving convergence of the results.

2.4 Elastic-plastic stress analysis - local strain limit

Based on the analysis performed in the elastoplastic regime, the principal stresses σ_1, σ_2, and σ_3, along with the von Mises equivalent stress σ_e, and the equivalent strain ε_{peq} were obtained for the previously defined loading conditions. From these results, it was possible to evaluate localized deformations, as described in item 5.3.3 of ASME VIII Division II [7]. To determine a pass/fail type strength criterion, the standard defines a limit for localized deformation according to Equation 2.

$$\varepsilon_L = \varepsilon_{Lu} \cdot \exp\left[-\left(\frac{\alpha_{sl}}{1+m_2}\right)\right]\left(\left\{\frac{(\sigma_1+\sigma_2+\sigma_3)}{3\sigma_e}\right\} - \frac{1}{3}\right), \tag{2}$$

The parameters m_2, α_{sl}, and ε_{Lu} are defined in table 5.7 of the standard for different types of materials. As a pass/fail criterion, it is defined that the sum of the equivalent plastic strain with the strains arising from the manufacturing process (ε_{cf}) must be less than or equal to the localized strain limit, as shown in Equation 3.

$$\varepsilon_{peq} + \varepsilon_{cf} \leq \varepsilon_L, \tag{3}$$

If this criterion is met, the analyzed component is in accordance with ASME VIII Division II [7] based on the localized deformations criterion. As a design consideration, deformations due to the manufacturing process were neglected. Thus, the pass/fail criterion was adopted as shown in Equation 4.

$$\varepsilon_L - \varepsilon_{peq} \geq 0, \tag{4}$$

In addition to this evaluation based on the difference between acting and limit deformations, the localized strain damage index was verified. In this procedure, the load path was divided into 58 load increments, including steps and sub steps. With this, the principal stresses, σ_1, σ_2, and σ_3, the equivalent stress, Δe_k, and the change in equivalent plastic strain relative to the previous load increment, $\Delta\varepsilon_{peqk}$, are calculated for each load increment. The deformation limit for the k-th load increment, ε_{Lk}, is calculated using Equation 2. The deformation damage limit for each load increment is calculated using Equation 5 and evaluated by the criterion in Equation 6, with the effects of forming deformation being disregarded.

$$De_k = \frac{\Delta\varepsilon_{peqk}}{\varepsilon_{Lk}}, \tag{5}$$

$$\sum_{k=1}^{M} De_k \leq 1, \tag{6}$$

3 Results

3.1 Elastic stress analysis method

The graph in Figure 3 presents the results obtained from the analysis of elastic stresses, condensing the values of membrane stress, bending stress, membrane + bending stress, peak stress, and total stress, along with the limits S (Sy/1.5) and Spl and Sps (Sy) for the 16 load paths applied to the valve.

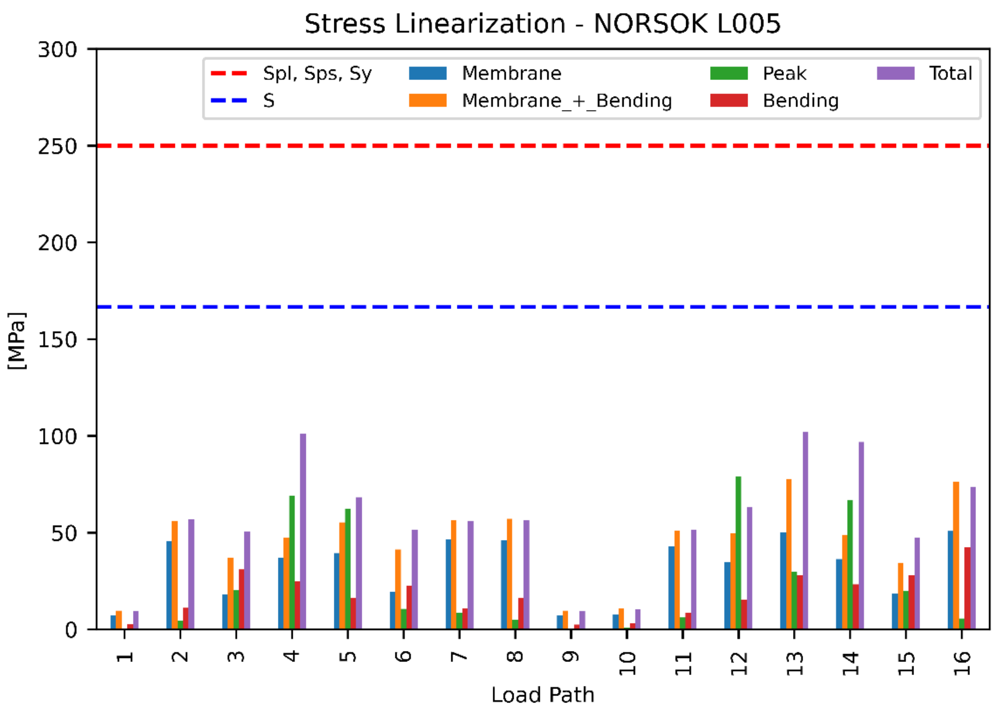

Figure 3 – Stress linearization and limits stress according to ASME VIII Division II [7]

As seen in the previous graph, all linearized stresses evaluated in the valve remain below the limits defined as Sy/1.5 and Sy. Therefore, the analysis was accepted with a pass condition for all load paths.

3.2 Elastic-plastic stress analysis

After defining the analysis conditions in the pre-processing stage, the processing was carried out using the ANSYS MAPDL 2022 R2 solver. As a result of the analysis, load step graphs were obtained, showing the number of iterations versus the number of subdivisions of the total load. Additionally, force convergence and force criterion graphs were generated. Both graphs were obtained through data analysis of the software outputs and are presented in Figure 4a and 4b, respectively.

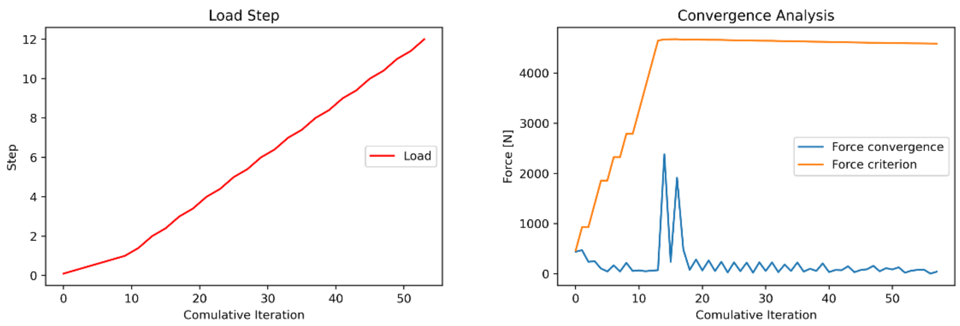

Figure 4 - a) Load Step Graph b) Force Convergence and Force Criterion Graph by Iteration

In graph 4b, force convergence measures the difference between the forces calculated in consecutive iterations and checks if this difference is below the pre-established limit. When the difference in forces between consecutive iterations is less than this limit, it is considered that the solution has converged.

Figure 5 presents the global deformations of the structure, where Figure 5a shows the deformation diagram on the geometry through a color map, while Figure 5b displays the graph of minimum, maximum, and average deformations as a function of iterations.

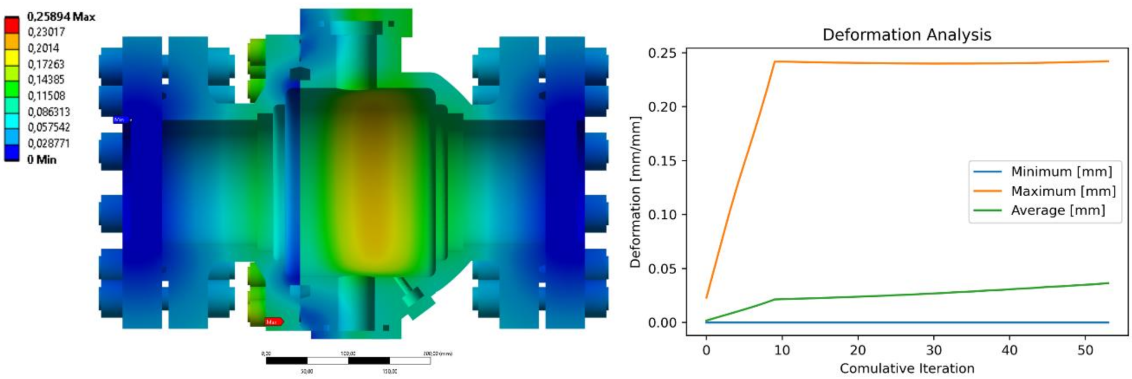

Figure 5 - a) Deformation Diagram b) Deformation Graph per Iterations

By relating the graphs from Figures 4a, 4b, and 5b, it is possible to verify a convergence of the results, as the 12 load steps were consistently satisfied, the force criterion parameter stabilized, as well as the force convergence, which not only stabilized but also tended towards 0 after a certain stage of the incremental analysis.

The graphs in Figure 6 demonstrate the behavior of the Von-Mises equivalent stresses, minimum, maximum, and average. It is possible to observe a gradual increase in stress until achieving convergence at a certain number of iterations, remaining stable after that point.

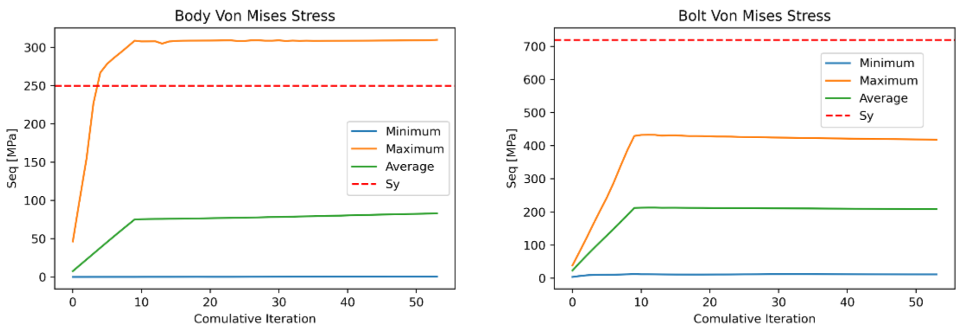

Figure 6 - Equivalent Von Mises Stress: a) Body and cover b) Bolts

It is worth noting that the elastic-plastic analysis assesses the convergence of results rather than a direct comparison with the material's yield limit, as done in an elastic analysis. This is because the elastic-plastic material model is applied, and the analysis seeks the structural stability under the action of load combinations.

3.3 Elastic-plastic stress analysis

Figure 7 presents the localized deformations criterion according to Equation 4.

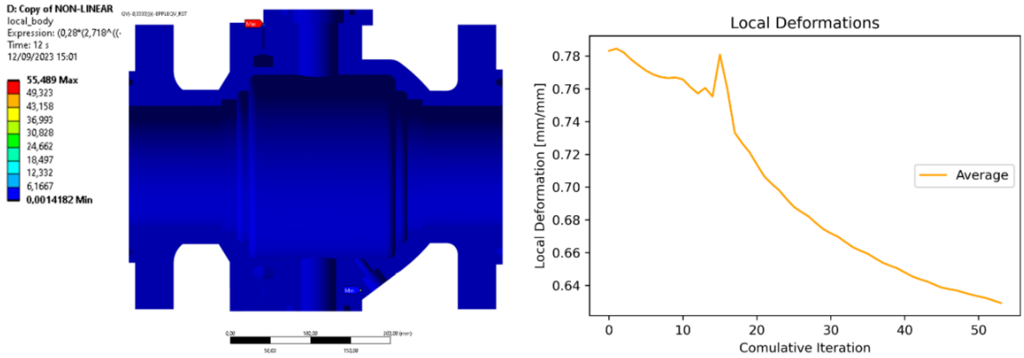

Figure 7 - Localized strain criterion distribution

When evaluating the criterion proposed in Equation 4, it is observed that all values at the points are positive, thus meeting the condition that there will be no localized deformations greater than the limit deformation proposed by ASME VIII Division II [7]. The damage index was also evaluated according to Equation 5, resulting in a value of 0.048, thus meeting the criterion of Equation 6.

4 Conclusions

Using NORSOK L005 [5], an initial geometry for the project was obtained. Next, we applied the analysis methodology outlined in ASME VIII Division II [7] to assess strength criteria. This analysis involved three steps: a linear elastic analysis using the stress linearization method, an elastic-plastic analysis, and a localized failure analysis using the elastic-plastic strain method. This meticulous, incremental, and iterative analysis enabled us to accurately understand the structure's behavior, ensuring convergence while evaluating deformations and stresses for various failure modes. Importantly, all results remained well within the safety limits specified by ASME VIII Division II [7]. This approach allowed us to evaluate the feasibility of utilizing the NORSOK L005 [5] standard in designing body and cover connection flanges. This strategy effectively reduced costs in ball valve design by minimizing mass. Notably, the NORSOK L005 [5] standard currently lacks specific guidelines for body and cover connection flanges, transforming this study into a scientific and technological research endeavor. Our study presents an optimization concept applicable to future industry projects. Furthermore, finite element analyses confirmed a substantial safety margin. This sets the stage for potential future investigations, such as optimizing the geometry as defined by NORSOK L005 [5]. Additionally, a comparative analysis of weight reduction can be conducted between the optimized model and one designed according to prevailing standards like ASME and API.

References

[1] MORAES, Osvaldo. Válvulas Industriais. Rio de Janeiro: Petrobras, 2005.
[2] ECOM. Setor de óleo e gás. 2020. Available in: bit.ly/3gHl8MB. Access in: 25 out. 2022.
[3] THE AMERICAN SOCIETY OF MECHANICAL ENGINEERS. ASME B16.34: Valves- -Flanged, Threaded, and Welding End. Eua: Asme, 2020. 228 p.
[4] AMERICAN PETROLEUM INSTITUTE. API SPECIFICATION 6D: Specification for Valves. 25ed. Eua: Api, 2021.
[5] NORSOK. L005: Compact flanged connections. 3 ed. Lysaker: Norsok, 2013.
[6] NORWAY, Standards. NORSOK standards. 2022. Available in: https://www.standard.no/en/sectors/energi-og-klima/petroleum/norsok-standards/. Access in: 25 out. 2022.
[7] THE AMERICAN SOCIETY OF MECHANICAL ENGINEERS. ASME BPVC-VIII-2: BPVC Section VIII-Rules for Construction of Pressure Vessels Division 2-Alternative Rules. Eua: Asme, 2019. 872 p.
[8] ALVES FILHO, Avelino, 1951- Elementos Finitos: A Base da Tecnologia CAE: Análise não linear / Avelino Alves Filho. – 6. Ed. – São Paulo: Érica, 2012.
[9] THE AMERICAN SOCIETY OF MECHANICAL ENGINEERS. ASME BPVC-II: BPVC Section II-Materials-Part D-Properties-(Customary). Eua: Asme, 2023. 1260 p.